RESEARCH ON THE IMPACT OF A PROJECTILE WITH COMPLEX KINEMATICS ON AN ARMOR PLATE

Daniela PINTILIE[1], Constantin PUICĂ[2],
Cătălin PÎRVULESCU[3], Cristina PUPĂZĂ[4]

The armor assures the protection of a combat vehicle and is crucial for the crew survival, but it affects the size, shape, and weight of the vehicle, as well as its mobility and combat ability. The research comprises an experimental and numerical study regarding the ballistic penetration and perforation phenomena of an Iron-Armco steel plate. The projectile performs a translation combined with a rotational movement and the effect of this kinematics at the impact is examined. Remarks regarding the improvement of the ballistic behavior were done.

Keywords: projectile, armor, impact, experiments, explicit dynamics, simulation.

1. Introduction

The armor is a physical protection barrier used in transportation or combat systems to reduce or to avoid damage caused by the enemy fire. The classical shielding uses metallic steel plates. Their considerable thickness protects the occupant, but the weight of the armored vehicle affects its maneuverability. The phenomena that occur during the projectile penetration into the structure are very important in the defense industry. During the process of penetration, the materials experience highly nonlinear dynamic behavior including strain and strain rate hardening, thermal softening and fracture [1].

Many researchers have investigated the mechanism of target's penetration. Liu et al [2] simulated in LS-DYNA a projectile with high rotating speed penetrating a moving vehicular door. Because of this movement the projectile turns and the ballistic trajectory migrates. Borvik [3] describes an experimental and numerical investigation on the ballistic penetration and perforation of Weldox 460F steel plates that consists of eight independently published parts that are

[1] Eng., Military Equipment and Technologies Research Agency of Bucharest, Romania , e-mail: danielapintilie07@gmail.com
[2] Eng., Military Equipment and Technologies Research Agency of Bucharest, Romania , e-mail: catalin.pirvulescu@yahoo.com
[3] Eng., Military Equipment and Technologies Research Agency of Bucharest, Romania , e-mail: catalin.pirvulescu@yahoo.com
[4] Prof., Department of Robotics and Manufacturing Systems, University POLITEHNICA of Bucharest, Romania, e-mail: cristina.pupaza@upb.ro

linked together through a synopsis. High velocity penetration of a 3-D rigid sharp impactor into a ductile layered target with air gaps between the plates was studied by Ben-Dor et al. [4]. They did some assumptions regarding the location of the projectile-target interaction.

The peculiarities of the penetration phenomenon for conical nose impactors were also studied. The ballistic performance of the target was independent on the air gap widths and on the sequence of the plates in the target. Murphy et al. [5] examined numerically and experimentally the effect of multiple jet punch targets.

In the case of kinetic projectiles, for a realistic assessment of the phenomenon, the following occurrences were analyzed: the propagation of the stress waves in the body of the projectile and in the armor, the exfoliation of the target on the opposite surface and the oscillatory movement of the armor plate, the penetration of the armor plate in the direct contact area between the projectile and the target, when plastic deformations followed by rupture occur [1]. Other studies, such as Almusallam et al. [6] refer to projectiles as well. Behner et al. [7] studied the impact of a golden hypervelocity projectile on the Silicon carbide (SiC) material. Turhan et al. [8], Serjouei [9] as well as Morka and Jacek [10] also analyzed the response of a SiC board against bullets of different sizes.

As a key component in the target-projectile system, the projectile is usually treated as a rigid body, ignoring the deformation of the projectile itself.

This paper comprises an experimental and numerical study that provides valuable information regarding the failure mode of the Iron-Armco plate and the detachment of splinters at impact of the copper shield from the steel core of the 7.62 mm projectile. The armor used in this study is placed on mobile equipments on the battlefield. The paper is structured in four parts. Software issues at impact simulations correlated with transitory and non-stationary phenomena are discussed in the context of the explicit dynamics approach. The third part of the work comprises an experimental case study that analyses the plate behavior during the impact and identifies the material failure. The main contribution is presented in the fourth part of the work, were the numerical simulation of a hit with a complex kinematics is described. The impact is simulated and examined taking into account the associated phenomena that occur as well as the observations taken during the experiments. The case study is summarized and conclusions are drew-up in the final chapter where future research viewports are also included.

2. Software issues regarding impact analysis

The impact of the projectile on the armor is a transitory phenomenon accompanied by high speed, heat transfer, elastic-plastic deformations or hydrodynamic flow. Therefore, the simulation must provide accurate results

regarding: the perforation depth, the speed of the projectile after it completely perforates the armor plate, the evaluation of the perforation time, the ability to describe the piercing of the armor by the projectile in given circumstances.

Explicit solvers comprise a powerful algorithm which assures that the simulation results follow closely the impact phenomenon, considers resonance or erosion and the high contact values, with directional rupture and cumulative effects. The procedure has the advantage that it does not form stiffness matrices, and thus significantly reduces the required computational resources. The solver allows error control and the calculation of large impact and deformation problems. One of the main advantages offered by the explicit solvers is that once the accelerations are known at time n, the velocities are calculated at time $n + 1/2$, and the displacements at time $n + 1$.

The equations solved by the explicit solver consider the conservation of mass, impulse, and energy in Lagrange coordinates. For each time step, these equations are explicitly computed for each element of the model, based on the input values at the end of the previous step. The simulation model was solved with ANSYS Explicit code to simulate the ballistic impact. The overall damage and residual velocity can also be accurately calculated. For the integration scheme the Leapfrog method is used [11]. After the computation of the forces at each node resulting from internal stress, contact or limit conditions, the nodal accelerations are obtained by dividing the force to the mass:

$$\ddot{x}_i = b_i + \frac{F_i}{m} \tag{1}$$

where $\ddot{x}_i$ are the components of the nodal acceleration (i = 1, 2, 3), F_i are the forces acting in the nodes, b_i are the components of the body acceleration and m is the mass.

Explicit solvers calculate the dynamic stress waves that need to be accurately modeled as they propagate across the mesh [11]. That is why the element size has to be carefully controlled by the user on the entire virtual model. An explicit special tetrahedral-element formulation included in the solver preprocessing system called nodal-based strain (NBS) eliminates shear locking, a problem encountered with traditional tetrahedral elements. A critical requirement for efficient and accurate explicit analysis is a high-quality mesh.

3. Experimental work

Experimental tests were carried out in the polygon in order to evaluate if an iron target of 5 mm thickness can be deployed as an effective shield. This plate is used on mobile equipment on the battlefield. Fig. 1 illustrates the experimental set-up with details regarding devices and dimensions and Fig. 2 presents the target attachment system.

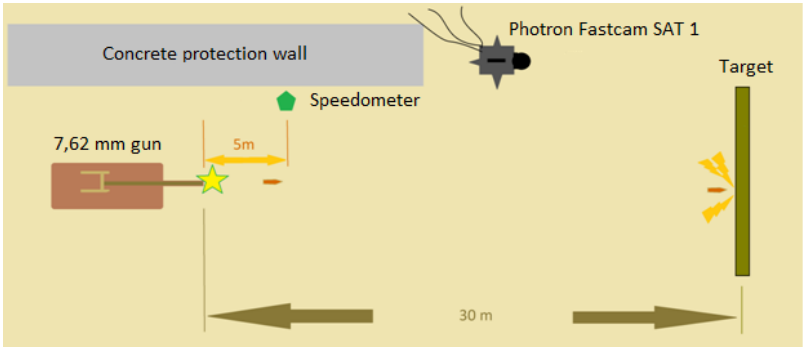

Fig. 1. Experimental set-up

The ammunition was a 7.62x39 mm perforating bullet. Before the sample was shot, the cartridges were held in a tempering chamber. The weapon was also a 7.62 mm caliber one. The distance between the tip of the ballistic bullet and target was 30 m. The average bullet impact velocity in the polygon was 715 m/s and the impact angle 0º.

Fig. 2. Target attachment during experiments

The dimensions of the armor plate are 500x500 mm. The effect of the shoot was the total perforation of the iron plate, which proved that a 5 mm thickness is an inappropriate value for the shield. The environmental conditions were the temperature of 5 °C, the pressure of 1.026 bar and the humidity of 70%.

The tests were completed to also monitor the armor plate behavior during the impact. As a result of the shooting, it was noticed that at impact the copper sleeve of the projectile was detached from the core. Results were recorded with a fastcam Photron SA1. This satisfies the image requirements of the most demanding applications in research and practice due to its sensitivity, speed and resolution. In order to match the variable region of interest to the aspect ratio of the theme, the device was adjusted to capture images at a frame rate of 40,000 fps.

Dead time between sequential frames is less than a microsecond. The fastcam SA1 can also be controlled remotely [12]. Frame sequences during impact were extracted from one of the gunshot movies as illustrated in Fig. 3, where the recorded time has a negative scale.

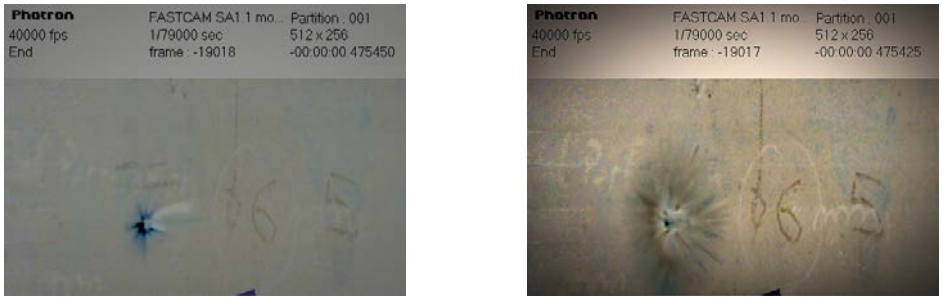

a. Impact at t= 0.47545s b. Impact at t=0.475425s

Fig. 3. Experimental results

The plastic deformation and the penetration of the armor at impact depend on the kinetic energy of the projectile, but also on the dimensions of the two parts. The strength of the armor plate during the experiments was evaluated by the ability to absorb the kinetic energy generated during impact, as well as its deformation around the impact zones. The target at the end of the experiments is illustrated in Fig. 4, proving that most of the projectiles have perforated the plate.

Fig. 4. The target at the end of experiment

The deformation of the plate is performed by the intertwining of several mechanisms: the Hopkins effect [1], the shock waves interference with the reflected waves, the initial pressure wave, the cross-cutting, the extrusion of a plug, specific to rigid armors; the reshaping of the impact surface in a star shape, specific to thicker bulkheads, the fragmentation with splinters, specific to fragile armors. While the perforation is a result of the high impact velocity, as well as the reduced thickness of the plate, splinters can destroy things behind the target. The behavior of the splinters is also a relevant phenomenon/consequence to be

observed in practice. The projectile passes through the armor, and the armor material undergoes a radial expansion over the perforation shaft.

Wherever wave interference occurs, the tension is essentially summed up, it becomes high and exceeds the ultimate tension value of the plate material. The micro-cracks turn into cracks that lead to the rupture of the material with splinters.

4. The numerical simulation of the impact

The numerical simulation aimed to describe the failure mode of the armor plate at impact. Because in the experimental stage most of the projectiles penetrated the 5 mm iron plate a primary conclusion was that it cannot be used as armor. That is why at this research stage a larger plate thickness was deployed, the material of the plate was reconsidered and even a lower initial speed than the average speed of the projectiles used during the experiments was chosen.

4.1 Model preparation

The material of the armor plate was this time an Iron-Armco material from the solver database [11]. The mechanical properties and the composition are specified in Table 1, exactly as in the solver library.

Table 1

Composition and properties of the Iron-Armco material [11]

Component Elements Properties	
Carbon, C	0.0500 %
Chromium, Cr	20.0 %
Iron, Fe	30.37 %
Manganese, Mn	4.00 %
Nickel, Ni	45.0 %
Niobium, Nb (Columbium, Cb)	0.150 %
Silicon, Si	0.400 %
Vanadium, V	0.0300 %
Elastic Properties	
Elastic Modulus	207 GPa
Poisson's Ratio	0.29
Shear Modulus	80 GPa
Bulk Modulus	164 GPa
Thermal Properties	
Density	7890 kg/m^3
Conductivity	73 W/mK
Specific Heat	452 J/kgK
Melting Temperature	1537.85 °C
Heat treatment Temperature	926.85 °C
Hardness : F-72 ROCKWELL	
Grain Size : 0.090- 0.150 mm	

The Iron-Armco material has excellent magnetic properties, high chemical and metallurgical purity, improved corrosion and oxidation resistance and good cold forming capacity. The material model used for the Iron-Armco plate is

Johnson Cook, which describes the behavior of the metallic materials at high deformation, high speed impact and high temperatures. The Johnson-Cook plasticity model is the most used among the temperature and strain-rate dependent models.

For a realistic simulation the 7.62 mm bullet model was downloaded from the free GrabCAD library (Fig. 5). The projectile is made of a STEEL 4340 core and a copper CU OFHC sheath form the solver database. These materials exhibit elastic behavior, shock response, plasticity, isotropic hardening, isotropic thermal softening and ductile fracture. Tests proved that CU OFHC and IRON Armco fail more ductile than 4340 steel.

a. 7.62 mm bullet b. virtual model

Fig. 5. Geometrical and computational model of the bullet

The width of the plate was 500 mm and the thickness was increased to 6 mm. The mesh strategy was the default algorithm used by the pre-processing system for all bodies, but a 40 mm diameter sphere of influence, comprising a very fine mesh around the impact area was included in the model (Fig. 6). The mesh size was $2.5 \cdot 10^{-4}$ m in the neighborhood of the contact area and a coarse mesh was generated for the rest of the model.

a. mesh around the impact area b. projectile and plate mesh detail

Fig. 6. The computational model

The initial kinetic conditions were: a reduced translational velocity of 650 m/s on the X-axis and an rotational velocity of 2094.4 rad/s (Fig. 7) in respect to the number of the guns joints in order to describe the combined roto-translational movement of the projectile, following the external ballistic rules. The gravitational acceleration, which slightly affects the outer ballistics of the shoot trajectory, has also been taken into account, along the negative Z axis.

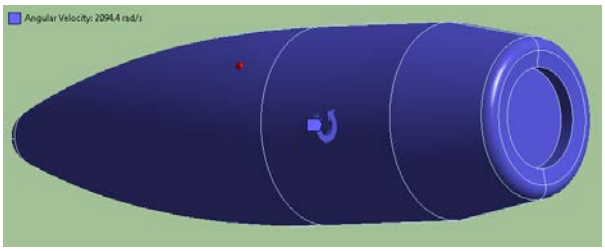

Fig. 7. Initial condition - 2094.4 rad/s applied angular velocity

Step control values during the solution were calculated taking into account the parameters of the shooting range. The step end time step was $1.221 \cdot 10^{-4}$s, the maximum number of cycles was 1007 and the minimum time step was set to 10^{-12}s.

4.2 Simulation results

The simulation proved that the projectile has fully penetrated the plate. The failure mode (Fig. 8a) is following the shape of the projectile. As a consequence of the impact, the copper shell (2) of the projectile detaches from the steel core (1), which remains almost intact.

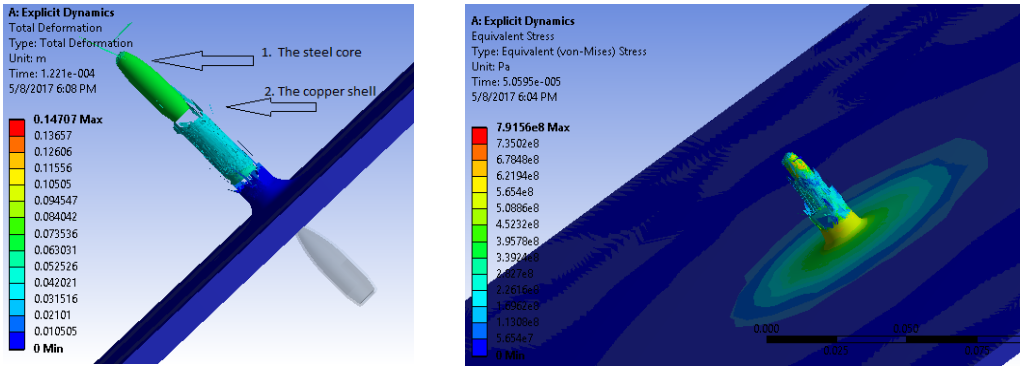

a. Total deformation at $t=1.221 \cdot 10^{-4}$ s b. Equivalent Von-Mises stress at $t=5.06 \cdot 10^{-5}$ s

Fig. 8. Simulation results

As expected, the most affected area of the armor plate is in the impact region, describing concentric circles from the center of impact to the exterior of the plate (Fig. 8b), showing that the equivalent von Mises stress of the armor plate increases. During the initial stage of the impact where the strain rate is very high, the failure of the target material appears. At this step, the bullet can be considered as a rigid body with very little deformation. During the second stage, the bullet

loses its kinetic energy. Very little penetration of the target takes place. The thermal prestressed material starts delaminating and a bulge in the rear face of the panel results. Finally the bullet starts penetrating the material. The equivalent von Mises plastic strain increases sharply. This was caused by the detachment of the copper shield from the steel core of the projectile (Fig. 9). The plastic deformation occurred and the total piercing of the plate can be observed. On the opposite side of the impact (B) splinters appeared that were detached in the radial direction. The failure mode of the armored plate can also been observed in Fig. 9, where the abnormal values of the equivalent plastic strain prove the rupture of the plate caused by the dislocation mechanics of shock-induced plastic behavior of the armor and explain the cause of splinters detachment.

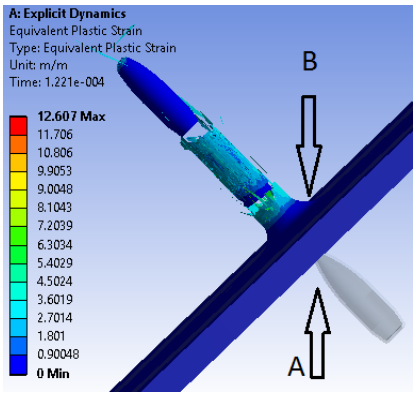

Fig. 9. Equivalent plastic strain at the end time of $1.221 \cdot 10^{-4}$s

The simulation model of the two elements, projectile and armor plate, was tuned both with the required analysis accuracy and the available computational resources. As a result of the impact, the projectile's speed dropped from 650 m/s to 499 m/s in $5 \cdot 10^{-5}$s and remained constant until the end of the simulation (Fig. 10).

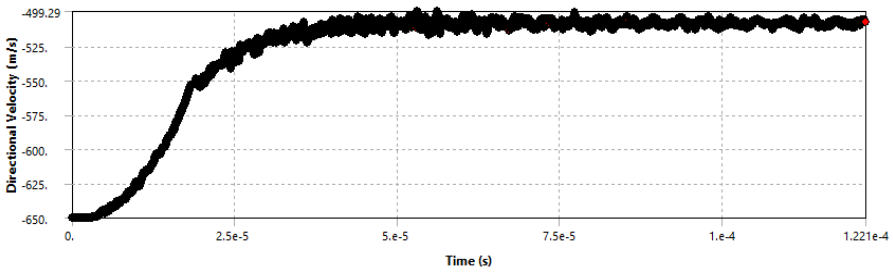

Fig. 10. Evolution of the velocity of the projectile on X axis

The acceleration of the projectile on the X axis (Fig. 11) exhibits variations during the simulation, but the highest value, up to $1.2 \cdot 10^8$ m/s^2 is recorded when the velocity decreases, which means that the impact with the penetrated projectile determined the failure (rupture) of the armor plate.

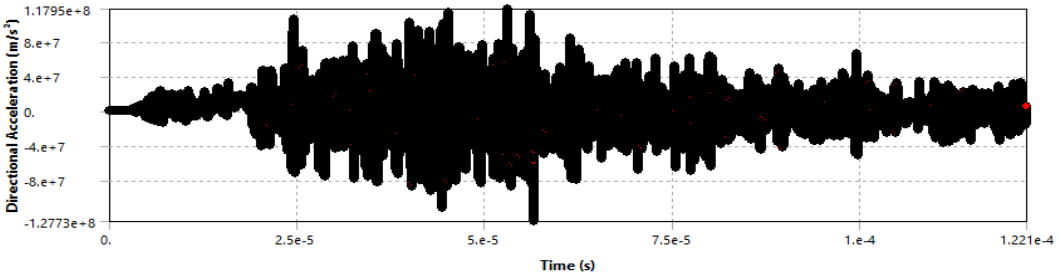

Fig. 11. Acceleration of the projectile on X axis

Analyzing the evolution of the impact from the velocity and acceleration graphs (Fig. 10 and 11), the time during which plastic deformations occur can be determined. It can also be concluded that when determining the thickness of the armor plate and its material, it is not sufficient to evaluate only the destructive potential of the weapon or the kinematics of the projectile, but it is very important to analyze the oscillations of the plate at impact.

5. Conclusion

Actions on the combat zone proved that not only at present, but also in the future, the armored technique remains the only one that smartly and efficiently combines occupant and fire protection.

This research comprises a two stage study on the phenomena that occur during the high speed impact between the projectile and an armor plate. Initial experiments were carried out in order to evaluate if an iron target of 5 mm thickness can be used as an effective shield plate on mobile combat systems. Since most of the plates were perforated during experiments a numerical simulation was conducted in the second stage of the research on an Iron-Armco plate with an increased thickness and superior mechanical properties. The speed was slightly reduced during the simulation in order to emphasize the failure modes of the materials during the impact between the projectile and the armor plate. A complex kinematics of the projectile and an explicit dynamic assessment were included in the simulation model. While experiments were useful in the early stages of the research, the simulation proved that only numerical procedures allow the researcher to evaluate in depth the behavior of the target material and the projectile during the impact, to include realistic kinematic details, to save valuable information at each time increment, to visualize the detached splinters

and to explain the failure modes of the materials. The main contribution of the paper consists in the relevant simulation procedure on a model with a complex kinematics.

In order to assure the occupant safety an augmented thickness of the plate is still needed and this affects the weight and the maneuverability of the armored vehicle. Future work will be focused on ceramic or composite materials and on a combination of metal-composite structures with reduced weight and appropriate mechanical properties.

Acknowledgement

This work has been funded by the European Social Fund from the Sectoral Operational Programme Human Capital 2014-2020, through the Financial Agreement with the title "Scholarships for entrepreneurial education among doctoral students and postdoctoral researchers (Be Antreprenor!)", Contract no. 51680/09.07.2019 - SMIS code: 124539.

R E F E R E N C E S

[1]. *Sorin Cristea*, "Contribuții la studiul comportării unor materiale de blindaj, la impactul cu proiectilele" (Contributions to the study of the behavior of armor materials at impact with projectiles), PhD Thesis (in Romanian), University Lucian Blaga, Sibiu, Romania, 2008.

[2]. *J. Liu, Y. Long, C. Jia, Q. Liu, M. Zhong, G. Song*, "Ballistic performance study on the composite structures of multi-layered targets subjected to high velocity impact by copper EFP", Composite Structures, **vol. 184**, 2018, pp. 484-496.

[3]. *T. Borvik*, "Ballistic Penetration and Perforation of Steel Plates", PhD Thesis, Norwegian University of Science and Technology, 2000.

[4]. *G. Ben-Dor, A. Dubinsky and T. Elperin*, "On the ballistic resistance of multilayered targets with air gaps", in Int. J. Solids Structures Vol. 35, No. 23. pp. 3097-3103, 1998.

[5]. *M.J. Murphy, D.W. Baum, R.M. Kuklo, S.C. Simonson*, "Effect of multiple and delayed jet impact and penetration on concrete target borehole diameter", Preprint UCRL-JC-139827, the article was submitted to 19th International Symposium. 2001.

[6]. *T.H. Almusallam, N.A. Siddiqui, R.A. Iqbal, H. Abbas*, "Response of hybrid-fiber reinforced concrete slabs to hard projectile", International Journal of Impact Engineering **vol. 58**, 2013, pp.17-30.

[7]. *T. Behner, D.L. Orphal, V. Hohler, C.E. Anderson Jr, R.L.Mason, D.W. Templeton, (2006),* "Hypervelocity penetration of gold rods into SIGN for impact velocities from 2.0 to 6.2 km/s", in Int. Journal of Impact Engineering, **vol.** 33, pp. 68-79.

[8]. *L. Turhan, Ö. Eksik, E.B. Yalçın, A. Demirural, T. Baykara, V. Günay*, "Computational simulations and ballistic verification tests for 7.62 mm AP and 12.7 mm AP bullet impact against ceramic metal composite armors", in Structures under Shock and Impact X, WITPress, pp. 379-388.

[9]. *A. Serjouei, R. Chi*, "An empirical model for the ballistic limit of bilayer ceramic metal armor", in Procedia Engineering, **vol. 75**, 2014, pp. 14-18.

[10]. *A. Morka, N. Jacek*, "Numerical analyses of ceramic/metal ballistic panels subjected to projectile impact", in Journal of KONES, **vol. 19**, 2012, pp. 465-472.
[11]. *** ANSYS Explicit Dynamics Analysis Guide, Release. 17, 2017.
[12]. https://photron.com/fastcam-sa1-1/